

# Exciton-phonon information flow in the energy transfer process of photosynthetic complexes

Patrick Rebentrost<sup>1,\*</sup> and Alán Aspuru-Guzik<sup>1,†</sup>

<sup>1</sup>*Department of Chemistry and Chemical Biology, Harvard University, 12 Oxford St., Cambridge, MA 02138*  
(Dated: May 29, 2022)

Non-Markovian and non-equilibrium phonon effects are believed to be key ingredients in the energy transfer in photosynthetic complexes, especially in complexes which exhibit a regime of intermediate exciton-phonon coupling. In this work, we utilize a recently-developed measure for non-Markovianity to elucidate the exciton-phonon dynamics in terms of the information flow between electronic and vibrational degrees of freedom. We study the measure in the hierarchical equation of motion approach which captures strong system-bath coupling effects and non-equilibrium molecular reorganization. We propose an additional trace-distance measure for the information flow that could be extended to other master equations. We find that for a model dimer system and the Fenna-Matthews-Olson complex that non-Markovianity is significant under physiological conditions.

The initial step in photosynthesis involves highly efficient excitonic transport of the energy captured from photons to a reaction center [1]. In most higher plants and other organisms such as green sulphur and purple bacteria this process occurs in light-harvesting complexes which consist of electronically coupled chlorophyll molecules embedded in a solvent and a protein environment [2]. Several recent experiments show that excitonic coherence can persist for several hundreds of femtoseconds even at physiological temperature [3]. These experiments suggest the hypothesis that quantum coherence may be biologically relevant for photosynthesis.

The challenging regime of intermediate coupling of the electronic to the vibrational degrees of freedom motivates the study of sophisticated master equations with non-Markovian effects. Several approaches have been taken, ranging from a polaron transformation [4], quantum state diffusion [5], generalized Bloch-Redfield [6], non-Markovian quantum jumps [7, 8], quantum path integrals (QUAPI) [9], to density matrix renormalization group (DMRG) [10]. After photoexcitation, the nuclear coordinates of a molecule will relax to new equilibrium positions, a phenomenon that is borne out by the time-dependent Stokes shift, that is the frequency shift between absorption and emission spectra. Redfield theory assumes that the phonon bath is always in thermal equilibrium and thus cannot capture this effect [11]. Ishizaki and Fleming employed the hierarchical equation of motion (HEOM) approach [12], which interpolates between the usual weak and strong (singular) exciton-phonon coupling limits and takes into account non-equilibrium molecular reorganization effects.

In this work, we study the non-Markovianity of the exciton transfer process by means of numerical simulation. Quantum mechanical time evolution under decoherence leads to transfer of information encoded in the electronic excited state to the vibrational degrees of freedom. Non-Markovianity can be characterized as the return of this information to the electronic degrees of freedom. To quantify the exciton-phonon information flow, we employ the state-of-the-art master equation approach by Ishizaki and Fleming and a newly-developed measure for non-Markovianity. The central question we will

answer is how much information is exchanged between excitonic and phononic degrees of freedom in that process and, specifically, how much information returns from the phonons to the exciton.

*Measure for non-Markovianity*— A recent area of research is the study of measures to characterize non-Markovianity [13, 14]. We utilize the readily applicable measure developed by Breuer and co-workers [13]. It is based on the quantum state trace distance:

$$D(\rho_1(t), \rho_2(t)) = \frac{1}{2} \text{Tr} \{ |\rho_1(t) - \rho_2(t)| \}, \quad (1)$$

where  $|A| = \sqrt{A^\dagger A}$ . This measure quantifies the distinguishability of two quantum states  $\rho_1$  and  $\rho_2$ . For a completely positive trace-preserving map  $E$  the trace distance is contractive, i.e.  $D(E(\rho_1), E(\rho_2)) \leq D(\rho_1, \rho_2)$  [15]. Time intervals in which  $D$  increases indicate non-Markovian information flow [13], in our case from the vibrational degrees of freedom back to the electronic degrees of freedom. In terms of the slope of  $D$ , i.e.  $\sigma(\rho_1(t), \rho_2(t)) = \frac{d}{dt} D(\rho_1(t), \rho_2(t))$ , this implies that  $\sigma > 0$  for these time intervals. Formally, a measure for non-Markovianity is defined by the following [13]:

$$\text{NM-ity} = \max_{\rho_1(0), \rho_2(0)} \int_0^\infty dt \mathcal{I}(\sigma(t)) \sigma(\rho_1(t), \rho_2(t)). \quad (2)$$

Here, the indicator function  $\mathcal{I}(x > 0) = 1$  ( $\mathcal{I}(x < 0) = 0$ ) monitors only the increasing part of the trace distance time evolution i.e. the information backflow. The optimization of the initial states in Eq. (2) obtains the maximally possible non-Markovianity of a particular quantum evolution. In the case of photosynthetic energy transfer, initial states are given by the particular physical situation and lead to smaller values for the non-Markovianity. We use both physical and optimized initial states in this work.

*Hierarchy equation of motion*— The Hamiltonian describing a single exciton in a complex with  $N$  molecules is given by  $H_e = \sum_{m=1}^N (\epsilon_m + \lambda) |m\rangle\langle m| + \sum_{m<n} J_{mn} (|m\rangle\langle n| + |n\rangle\langle m|)$ . The site energies  $\epsilon_m$ , and couplings  $J_{mn}$  are obtained from detailed quantum chemistry studies and/or fitting of experimental data. The set of states  $|m\rangle$  denotes the site basis. The reorganization energy  $\lambda$  is the energy difference of the non-equilibrium phonon state after

\* rebentr@fas.harvard.edu

† aspuru@chemistry.harvard.edu

Franck-Condon excitation and the equilibrium phonon state and is assumed to be the same for each site. The superoperator corresponding to  $H_e$  is  $\mathcal{L}_e \rho = [H_e, \rho]$ . The Hamiltonian for the phonon environment is  $H_{\text{ph}} = \sum_i \hbar \omega_i (p_i^2 + q_i^2) / 2$ , where  $\omega_i$ ,  $p_i$ , and  $q_i$  are the frequency, dimensionless momentum and position operators of the phonon mode  $i$ . The coupling of the electronic degrees of freedom to the phonons is given by the Hamiltonian  $H_{\text{ex-ph}} = \sum_m V_m (\sum_i g_i q_i)_m$ , with  $V_m = |m\rangle\langle m|$  and where we assume that site-energy fluctuations dominate, the bath degrees of freedom at each site are uncorrelated, and the coupling constants to the respective modes are given by the constants  $g_i$ . The spectral density, which describes the coupling strength of exciton to particular phonon modes, is given by  $J(\omega) = 2\lambda\gamma\omega / (\omega^2 + \gamma^2)$ . Perhaps the most relevant parameter, the bath dissipation rate  $\gamma$ , is related to the bath correlation time by  $\tau_c = 1/\gamma$ . The equation of motion for the reduced single-exciton density matrix  $\rho$  is obtained by tracing out the less relevant phonon degrees of freedom and utilizing Wick's theorem for the Gaussian fluctuations, leading to a non-perturbative hierarchy of system and auxiliary density operators (ADOs) [12]:

$$\begin{aligned} \frac{\partial}{\partial t} \sigma^{\mathbf{n}}(t) = & - \left( i\mathcal{L}_e + \sum_{m=1}^N n_m \gamma \right) \sigma^{\mathbf{n}}(t) \\ & + \sum_{m=1}^N \phi_m \sigma^{\mathbf{n}_{m+1}}(t) + \sum_{m=1}^N n_m \theta_m \sigma^{\mathbf{n}_{m-1}}(t). \end{aligned} \quad (3)$$

The system density matrix is the first member of the hierarchy  $\rho(t) = \sigma^{\mathbf{0}}(t)$ . The other members of the hierarchy are arranged in tiers and indexed by  $\mathbf{n} = (n_1, \dots, n_N) \geq 0$ , where a single tier is given by all elements where  $\sum_m n_m$  is constant. The notation  $\mathbf{n}_{m\pm 1} = (n_1, \dots, n_m \pm 1, \dots, n_N)$  is introduced. The superoperators in the high temperature regime  $\hbar\gamma\beta < 1$  are  $\phi_m \sigma^{\mathbf{n}} = i[V_m, \sigma^{\mathbf{n}}]$  and  $\theta_m \sigma^{\mathbf{n}} = i(2\lambda/\beta\hbar^2 [V_m, \sigma^{\mathbf{n}}] - i\lambda\gamma/\hbar \{V_m, \sigma^{\mathbf{n}}\})$  and act on system and ADOs, where  $\{, \}$  is the anticommutator. Initially, all the hierarchy members are zero, which corresponds to the electronic ground state phonon equilibrium configuration. For numerical propagation, the hierarchy is truncated based on the criterion  $\sum_m n_m \gg \frac{\omega_e}{\gamma}$ , where  $\omega_e$  is a characteristic frequency of  $\mathcal{L}_e$ . We assume that this condition is satisfied when the  $\sum_m n_m$  is by a factor 5 larger than  $\frac{\omega_e}{\gamma}$ .

The representation of the hierarchy equation of motion in Eq. (3) is not unique. It can be advantageous to expand the hierarchy in a set of *normalized* auxiliary systems [16]. Redefining the ADOs as  $\tilde{\sigma}^{\mathbf{n}}(t) = (\prod_m n_m |c_0|^{-n_m})^{-1/2} \sigma^{\mathbf{n}}(t)$  and rescaling the superoperators as  $\phi_m \sigma^{\mathbf{n}_{m+1}} = \sqrt{(n_m+1)} |c_0| \phi_m \tilde{\sigma}^{\mathbf{n}_{m+1}}$  and  $n_m \theta_m \sigma^{\mathbf{n}_{m-1}} = \sqrt{n_m} |c_0| \theta_m \tilde{\sigma}^{\mathbf{n}_{m-1}}$ , with  $c_0 = (2\lambda/\beta\hbar^2 - i\lambda\gamma/\hbar)$  in the high temperature regime, leads to a more balanced EOM and can lead to a lower requirement in terms of the number of ADOs. The rescaled representation is useful for simulating large systems such as the FMO complex and for studying the ADOs themselves, as follows.

To characterize the information flow from the point of view of the non-Markovian degrees of freedom, we propose another measure based on the trace distance. The auxiliary systems

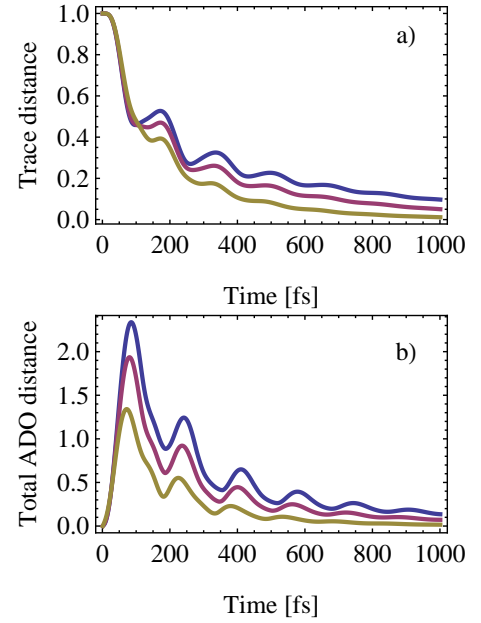


FIG. 1. (a) Trace distance of the states  $\rho_1 = |1\rangle\langle 1|$  and  $\rho_2 = |2\rangle\langle 2|$  as a function of time for a two-site system (dimer) in the hierarchy equation of motion model. The trace distance evolves from maximally distinguishable ( $= 1$ ) for the initial states to indistinguishable ( $= 0$ ) for the thermal equilibrium state. At intermediate times, the trace distance increases, which is due to a reversal of the information flow. Various bath correlation times are shown, 150 fs (blue), 100 fs (red), and 50 fs (yellow). For long correlation times, that is, a bath with more memory, the regions of increasing trace distance are more pronounced. (b) The ADO distance  $D_{\text{ADO}}^{\text{tot}}$  illustrates the information content in the non-Markovian degrees of freedom of this model for the same system, initial states, and bath correlation times as in (a). The anticorrelated oscillations of the two figures clearly show the information flow between the system and the NM degrees of freedom.

describe perturbations on the time-evolved excitonic state due to the phonon environment. This separation into system and auxiliary degrees of freedom implies a quantification of the information content of the auxiliary systems at a given point in time:

$$D_{\text{ADO}}^{\text{tot}}(t) = \sum_{\mathbf{n} \neq \mathbf{0}} D(\tilde{\sigma}_1^{\mathbf{n}}(t), \tilde{\sigma}_2^{\mathbf{n}}(t)). \quad (4)$$

This measure depends on the electronic initial states and, importantly, uses the normalized ADOs. Although the  $\tilde{\sigma}^{\mathbf{n}}(t)$  are not quantum states for  $\mathbf{n} \neq \mathbf{0}$ , the trace distance nevertheless measures differences of these operators arising from the different initial states. This measure could in principle be extended to other families of master equations that employ auxiliary degrees of freedom.

*Results for a dimer*— In this section, a two-molecule system, or dimer, is studied in terms of the measure for non-Markovianity, using, if not otherwise mentioned, the regular hierarchy equation of motion approach Eq. (3) and scanning over the parameters of the model. As standard parameters, we use the site energies  $\epsilon_1 = 0$ ,  $\epsilon_2 = 120/\text{cm}$ ,

and the coupling  $J = -87.7/\text{cm}$ . This corresponds to the strongly-coupled bacteriochlorophyll site 1 and 2 subsystem of the Fenna-Matthews-Olson complex. Along the lines of the discussion in [12], the standard bath correlation time is taken from 50 fs to 150 fs. We assume ambient temperature  $T = 288 \text{ K}$  (200/cm). The main results use 40 tiers (819 ADOs), and Eq. (3) is integrated up to maximally 20 ps.

First, in Fig. 1 (a), we investigate the time evolution of the trace distance in Eq. (1) for the dimer system at reorganization energy  $\lambda = 20/\text{cm}$ . We choose the two initial states  $\rho_1 = |1\rangle\langle 1|$  and  $\rho_2 = |2\rangle\langle 2|$  and the standard parameters given above, while varying the bath dissipation rate. One can see clear non-Markovian revivals in the time intervals at around 150 fs and around 300 fs, borne out by increases in the trace distance. For larger correlation time of the bath of  $\tau_c = 150 \text{ fs}$  these revivals are more pronounced. A bath excitation is more likely to return to the system instead of being dissipated away rapidly, as occurs in the case of smaller correlation time  $\tau_c = 50 \text{ fs}$ .

In Fig. 1 (b), we investigate the time evolution of the ADO distance measure in Eq. (4) for the same system, using the normalized auxiliary systems. At small times, the ADOs are all zero, thus  $D_{\text{ADO}}^{\text{tot}} = 0$ , while at long times the system and ADOs converge to the thermal equilibrium and all information about the initial states is dissipated. At intermediate times, one finds strong information flow between system and the non-Markovian degrees of freedom, which is borne out by the anticorrelated oscillations in (a) and (b), respectively. For this, note the dips at around 150 fs and around 300 fs in (b). Additionally, the information content in the ADOs is smaller when the bath dissipation rate is larger.

The computation of the non-Markovianity measure in Eq. (2) involves an optimization of the initial states. On the one hand, the following results use the two initial states  $\rho_1 = |1\rangle\langle 1|$  and  $\rho_2 = |2\rangle\langle 2|$  as above, but on the other hand, compare to a systematically-optimized pair of initial states. One initial state is chosen out of 50 pure states on the Bloch sphere. This leads to a total number of 1225 independent pairs of states in the optimization. (The state optimization itself is performed with 20 tiers of ADOs.)

We now proceed to scan the NM-ity measure over the parameters of the model, beginning with the system parameters, the site energy difference and the chromophoric coupling. First, the NM-ity is strongly dependent on the chromophoric coupling, see Fig. 2 (a). At zero coupling, the molecules are independent and the NM-ity is zero; the two initial states remain perfectly distinguishable. At non-zero coupling, the dynamics shows increasing NM revivals, while both initial states converge to the same thermal equilibrium state. Second, with respect to the site energy difference, the dependence of the NM-ity weakly slopes downward, see Fig 2 (b). As the energy difference increases the coupling becomes less significant and the molecules become more independent. This leads to decreased NM-ity.

Next, we investigate the role of the bath parameters. First, as mentioned before, the bath correlation time crucially affects the memory of the bath and the information back flow to the system. In Fig. 2 (c), we show the NM-ity mea-

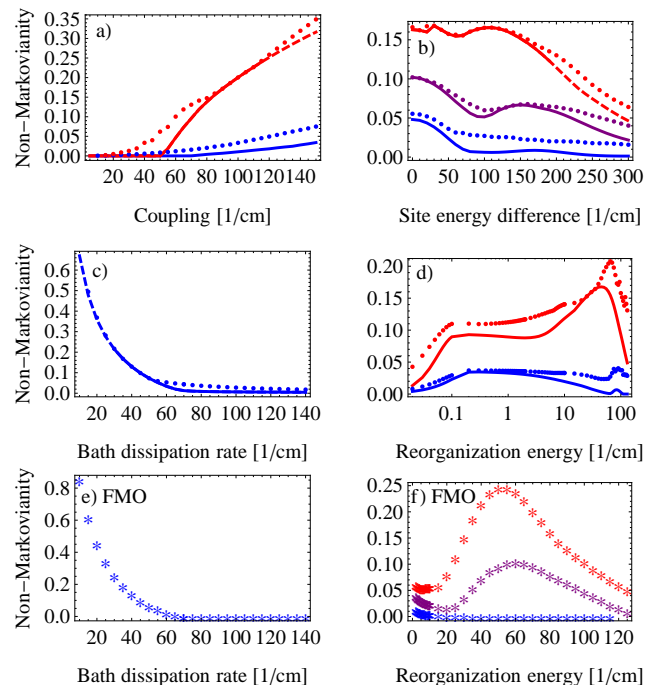


FIG. 2. Non-Markovianity as a function of the parameters of a dimer system, a)-d), and the Fenna-Matthews-Olson complex, e) and f), in the hierarchy equation of motion approach. For the dimer: a) coupling  $J_{12}$ , b) site energy difference  $\epsilon_2 - \epsilon_1$ , c) bath dissipation rate  $\gamma$  (which is related to the bath correlation time by  $\gamma = 1/\tau_c$ ), and d) reorganization energy  $\lambda$ . The solid lines are calculations performed with the initial states being  $\rho_1 = |1\rangle\langle 1|$  and  $\rho_2 = |2\rangle\langle 2|$  while the dots are calculations performed with optimized initial states. The dashed part of the lines indicates that a parameter was scanned beyond the validity of the equation based on the truncation condition. For the FMO complex: e) bath dissipation rate and f) reorganization energy. In all figures, except in c) and e), we use the different bath correlation times: 50 fs (blue), 100 fs (purple), and 150 fs (red).

sure as a function of the inverse bath correlation time, i.e. the bath dissipation rate. A longer  $\tau_c$  leads to more non-Markovianity, because a sluggish bath keeps the memory of excitations much longer and the information is able to return back to the electronic degrees of freedom. Second, the other significant bath parameter, the reorganization energy, is a measure of the non-equilibrium character of the phonon bath in the excited state. In Fig. 2 (d), we show the NM measure as a function of the reorganization energy. At zero  $\lambda$ , which essentially means no coupling to the phonons, the unitary dynamics obviously shows zero non-Markovianity. At weak  $\lambda$ , we observe a NM-ity of around 0.1 at  $t_c = 150 \text{ fs}$ , which is completely neglected by Redfield theory. At intermediate  $\lambda$  of around 40/cm, close to the physiological values of the Fenna-Matthews-Olson complex, the NM-ity is maximal, showing a value of around 0.2. At large  $\lambda$ , the regime of incoherent transport [12], the NM-ity vanishes.

*Results for the Fenna-Matthews-Olson complex*— We now investigate the exciton-phonon information flow in the Fenna-Matthews-Olson complex. The FMO complex is found in green sulphur bacteria, where it connects the antenna complex

with the reaction center during the energy transfer process. The FMO complex is a trimer with seven bacteriochlorophyll (BChl) molecules in each subunit and with one additional BChl molecule shared between the units. We implement the hierarchy equation of motion for the seven sites ( $N = 7$ ), using the method for rescaling the auxiliary systems as discussed above and in [16]. As was shown recently [17], with four tiers (329 ADOs) the coherent population dynamics can be accurately simulated, but due to the reduced number of ADOs, we expect to minimally overestimate the NM-ity. We use the initial states  $\rho_1 = |1\rangle\langle 1|$  and  $\rho_2 = |2\rangle\langle 2|$ . First, the scan of  $\gamma$  obtains a strong dependence similar to the dimer system, see Fig. 2 (e). Second, the scan of the reorganization energy obtains a maximum at around  $\lambda = 55/\text{cm}$  with the NM-ity being 0.2 at  $\lambda = 35/\text{cm}$  and  $\tau_c = 150$  fs, see Fig. 2 (f). The results suggest that non-Markovian effects should play a significant role in the function of the Fenna-Matthews-Olson complex.

*Conclusion*— The theoretical and experimental characterization of photosynthetic light-harvesting complexes in terms of non-Markovianity, as e.g. defined in the recent work

[13, 14], can lead to a greater understanding of the exciton dynamics in these systems. In principle, the recently proposed ultrafast quantum process tomography protocol extracts a full characterization of the quantum map [18], and could thus be used for the experimental side of this task. However, experiments specifically designed to extract a particular observable, such as in our case the NM-ity measure, could be carried out with a reduced number of experimental requirements. Future work will investigate analytically and numerically how to efficiently extract the non-Markovianity from the phase-matched signal observed in four-wave mixing experiments.

To summarize, we have shown numerically that there is a considerable non-Markovian information flow between electronic and phononic degrees of freedom of light-harvesting chromophoric systems under physiological conditions, utilizing a realistic model for systems such as the Fenna-Matthews-Olson complex. The results suggest that non-Markovianity plays a significant role in photosynthetic energy transfer.

The authors are grateful to J. Piilo, C. Rodriguez-Rosario, S. Saikin, and J. Zhu for insightful discussions. The authors acknowledge funding from DOE, DARPA, and computational resources through Harvard Research Computing.

- 
- [1] R. E. Blankenship, *Molecular Mechanisms of Photosynthesis*, 1st ed. (Wiley-Blackwell, 2002) p. 336.
- [2] Y.-C. Cheng and G. R. Fleming, *Annual Review of Physical Chemistry* **60**, 241 (2009).
- [3] G. S. Engel, T. R. Calhoun, E. L. Read, T.-K. Ahn, T. Mancal, Y.-C. Cheng, R. E. Blankenship, and G. R. Fleming, *Nature* **446**, 782 (2007); H. Lee, Y.-C. Cheng, and G. R. Fleming, *Science* **316**, 1462 (2007); G. Panitchayangkoon, D. Hayes, K. A. Fransted, J. R. Caram, E. Harel, J. Wen, R. E. Blankenship, and G. S. Engel, *Proceedings of the National Academy of Sciences of the United States of America* **107**, 1 (2010); E. Collini, C. Y. Wong, K. E. Wilk, P. M. G. Curmi, P. Brumer, and G. D. Scholes, *Nature* **463**, 644 (2010).
- [4] S. Jang, Y.-C. Cheng, D. R. Reichman, and J. D. Eaves, *The Journal of Chemical Physics* **129**, 101104 (2008).
- [5] J. Roden, A. Eisfeld, W. Wolff, and W. Strunz, *Physical Review Letters* **103**, 3 (2009).
- [6] J. Wu, F. Liu, Y. Shen, J. Cao, and R. J. Silbey, <http://arxiv.org/abs/1008.2236> (2010).
- [7] J. Piilo, S. Maniscalco, K. Härkönen, and K.-A. Suominen, *Physical Review Letters* **100**, 1 (2008).
- [8] P. Rebentrost, R. Chakraborty, and A. Aspuru-Guzik, *The Journal of Chemical Physics* **131**, 184102 (2009).
- [9] M. Thorwart, J. Eckel, J. Reina, P. Nalbach, and S. Weiss, *Chemical Physics Letters* **478**, 234 (2009).
- [10] J. Prior, A. Chin, S. Huelga, and M. Plenio, *Physical Review Letters* **105**, 1 (2010).
- [11] A. Ishizaki and G. R. Fleming, *The Journal of Chemical Physics* **130**, 234110 (2009).
- [12] A. Ishizaki and G. R. Fleming, *The Journal of Chemical Physics* **130**, 234111 (2009); *Proceedings of the National Academy of Sciences of the United States of America* **106**, 17255 (2009).
- [13] H.-P. Breuer, E.-M. Laine, and J. Piilo, *Physical Review Letters* **103**, 1 (2009).
- [14] M. Wolf, J. Eisert, T. Cubitt, and J. Cirac, *Physical Review Letters* **101**, 1 (2008); A. K. Rajagopal, A. R. U. Devi, and R. W. Rendell, <http://arxiv.org/abs/1007.4498> (2010); A. Rivas, S. Huelga, and M. Plenio, *Physical Review Letters* **105**, 1 (2010).
- [15] M. A. Nielsen and I. L. Chuang, *Quantum Computation and Quantum Information*, 1st ed. (Cambridge University Press, 2000).
- [16] Q. Shi, L. Chen, G. Nan, R.-X. Xu, and Y. Yan, *The Journal of Chemical Physics* **130**, 084105 (2009).
- [17] J. Zhu, S. Kais, P. Rebentrost, and A. Aspuru-Guzik, *Journal of Physical Chemistry B* (in press) (2010).
- [18] J. Yuen-Zhou, M. Mohseni, and A. Aspuru-Guzik, <http://arxiv.org/abs/1006.4866> (2010).